Combustion Science and Technology
Publication details, including instructions for authors and subscription information:
http://www.tandfonline.com/loi/gcst20

NUMERICAL ANALYSES FOR RADIATIVE IGNITION AND TRANSITION TO FLAME SPREAD OVER A HORIZONTALLY ORIENTED SOLID FUEL IN A GRAVITATION FIELD

PEI-HSUN LIN [a] , WEI-FON FAN [a] & CHIUN-HSUN CHEN [a]
[a] Department of Mechanical Engineering , National Chiao-Tung University , HsinChu, Taiwan, R.O.C
Published online: 09 Jun 2010.

To cite this article: PEI-HSUN LIN , WEI-FON FAN & CHIUN-HSUN CHEN (2001) NUMERICAL ANALYSES FOR RADIATIVE IGNITION AND TRANSITION TO FLAME SPREAD OVER A HORIZONTALLY ORIENTED SOLID FUEL IN A GRAVITATION FIELD, Combustion Science and Technology, 173:1, 47-74

To link to this article: http://dx.doi.org/10.1080/00102200108935844

Combust. Sci. and Tech., 173:47–74, 2001

0010-2202/01 $12.00 + .00

NUMERICAL ANALYSES FOR RADIATIVE IGNITION AND TRANSITION TO FLAME SPREAD OVER A HORIZONTALLY ORIENTED SOLID FUEL IN A GRAVITATION FIELD

PEI-HSUN LIN, WEI-FON FAN, AND CHIUN-HSUN CHEN*

Department of Mechanical Engineering,
National Chiao-Tung University, HsinChu, Taiwan, R.O.C.

This study numerically investigates the ignition behaviors of horizontal-oriented cellulosic materials subjected to radiant heat flux under a natural convective environment. This process can be divided into two stages: (1) the heating-up stage, during which the maximum temperature increases with time and (2) the flame development stage, consisting of the ignition and transition processes. The ignition process is marked with a sharp increase in maximum temperature. Meanwhile, the flame is in a transition from a premixed flame into a diffused one. In the transition process, the flame propagates upstream, forming a so-called opposed flame spread. There is a time lag between solid fuel pyrolysis and the gas-phase chemical reaction. The pyrolysis front overtakes the flame front in the initial heating-up process. As soon as the flammable mixture ahead of the flame front is ignited, the flame moves forward quickly, moving ahead of the pyrolysis front. The ignition delay time is shorter for a horizontal solid fuel than for a vertical solid fuel under the same environment, because the resultant high-temperature region is not cooled and the flammable mixture is not diluted by the induced flow in a horizontal solid fuel. For the effect of changing gravity, the ignition delay time decreases with a decrease in gravity level, owing to the smaller induced flow velocity.

Received 6 July 2001; accepted 3 December 2001.

The authors wish to express their appreciation for financial support from Engineering Division of National Research Council of Taiwan, R.O.C., under grant, NSC 89-2212-E-009-049.

*Address correspondence to chchen@cc.nctu.edu.tw

Keywords: radiative ignition, flame spread, solid fuel, gravitational field, horizontally oriented

INTRODUCTION

This study investigated the ignition and transition to flame spread behaviors over a horizontal solid fuel, subjected to a radiant heat flux under a natural convective environment in a normal gravitational field. This study was motivated by Lin and Chen (2000), who studied the corresponding combustion phenomena over a vertically oriented solid fuel in the same environment. In that work, the fuel vapor mass fraction distribution in the gas phase was determined mainly by the induced-flow features, implying that the ignition behavior is strongly affected by the naturally convective flow motion, whose characteristics depend on the solid-fuel orientation. Since the induced flow motion over a horizontal solid fuel is expected to be different from one over a vertical solid fuel, the ignition and subsequent spreading flame are also expected to be different. In addition, the variation in gravity level changes the intensity of the buoyant force, which in turn affects the induced flow motion. Previous studies, such as Chen and Yang (1998), Duh and Chen (1991) and West, Bhattacharjee, and Altenkirch (1992), confirmed that the magnitude of gravity indeed plays an important role in an opposed flame-spread process. However, how the solid-fuel orientation and gravity level influence the ignition characteristics have seldom been investigated in detail.

For problems associated with solid fuel ignition characteristics, experiments performed by Kashiwagi (1982) showed that the ignition delay time was shorter for a horizontal sample than for a vertical sample. The minimum external radiative flux required for ignition to occur for the horizontal sample was less as well. In a quiescent microgravity environment, Nakabe et al. (1994) showed that ignition occurs with a 30 percent oxygen concentration, and that the transition from ignition to flame spread did not occur until the oxygen concentration reached 50 percent for a thermally thin cellulosic material. Mcgrattan et al. (1996) found that the ignition delay time depends mainly on the peak flux of the external radiation, while the transition time to flame spread depends mainly on the broadness of the flux distribution. They also found that an imposed wind up to 5 cm/s enhances the strength of the opposed flame spread rate due to the greater supply of oxygen. A numerical study by Nakamura, Yamashita, and Takeno (2000) investigated the behavior of the gas-phase

ignition over a horizontal thin solid fuel under various ambient oxygen concentrations and gravity levels. In the gravity region (0 g $\sim$ 0.25 g), the ignition delay time decreases slightly with the increasing of gravity. When the gravity is between 0.25 g and 1 g, the ignition delay time rises with the gravity. If the ambient oxygen concentration is below $Y_{ox} = 0.68$, the ignition delay time will decrease with the ambient oxygen concentration, but beyond $Y_{ox} = 0.68$ the influence is insignificant. The experiment by Ito and Kashiwagi (1986) investigated temperature distributions inside a thermally thick slab of PMMA for a downward flame spread using a holographic interferometry technique. The results indicated that the visible flame front extends ahead of the vaporization front as the surface temperature reaches the vaporization temperature of about 380°C. For related literature on this subject, the reader can refer to Lin and Chen (2000). This information is not repeated here.

Although fires are generally driven by natural convection, until now no model is sophisticated enough to describe the complicated interaction between the gas and solid phases during the ignition process under a natural convective environment in a gravitational field. In light of the above situation, this study developed a time-dependent combustion model to simulate and study the radiative ignition processes and subsequent transition to flame spread over a horizontally oriented solid fuel. The predicted results are then used to compare against the vertical solid fuel results obtained previously by Lin and Chen (2000) to distinguish the respective controlling mechanisms. A parametric study based on the gravity level changes is also provided to study its influence on the ignition and flame spread over a thick solid fuel.

MATHEMATICAL MODEL

Figure 1 presents the schematic configuration of a two-dimensional ignition and the subsequent transition to flame spread over a horizontally oriented solid fuel, the boundary conditions, and the computational domain. Since a symmetrical condition is applied in the middle plane, the computations are carried out on the half plane; $x \leq 0$. At time $t < 0$, the flow field is quiescent. When $t \geq 0$, a vertical downward external heat flux in a Gaussian distribution is imposed on the solid surface and the position of $x = x_{max}$ is located at the gas-phase symmetry plane, coincident with the peak of the incident Gaussian-typed heat flux; see Figure 1. Then, the solid is heated and its temperature rises with pyrolysis occurring.

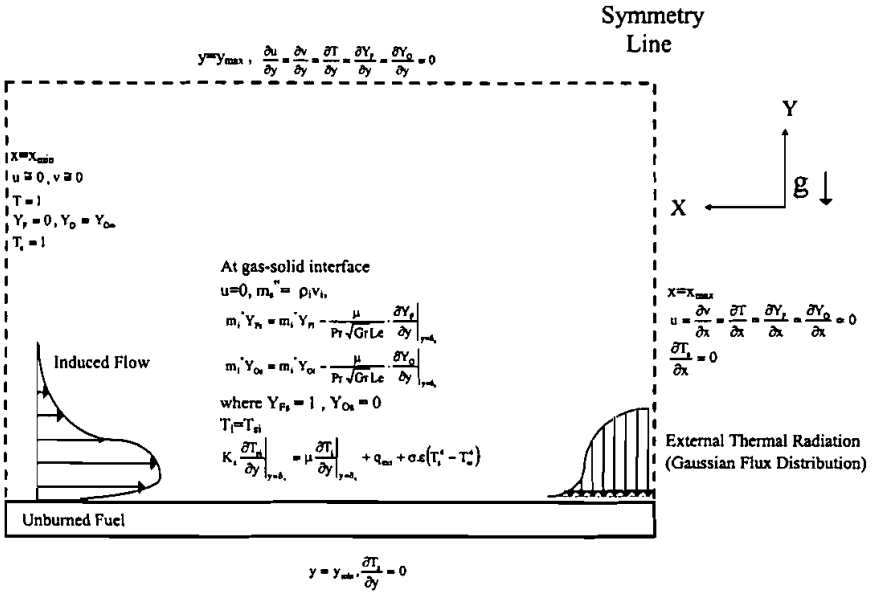

Figure 1. Configuration of radiative ignition of a horizontal solid fuel.

Simultaneously, the hot surface transfers heat to the gas layer adjacent to it. A rise in the gas-phase temperature causes a change in the gas density, which results in a fluid motion to build a natural convection near the fuel plate. This flow field cannot be prescribed in advance but is provided as part of the solution.

Except for the gravity orientation, the structures and assumptions for the combustion model are essentially the same as those proposed in the study of Lin and Chen (2000). Therefore, a detailed description is not given here. Table 1 summarizes the dimensionless, unsteady governing equations for continuity, momentum, energy, and species in the gas phase.

This numerical scheme adopts the SIMPLE algorithm (1980), which was described thoroughly by Lin (1999). A series of numerical tests was carried out in advance. According to these tests, the solution obtained by a grid distribution of 129×159 (corresponding to a nondimensional computational domain of 222.5×296.8) with a time step $\Delta t = 10$ (equal to 0.0548 sec dimensionally) can be acceptable. This grid-size and time-step set is also regarded as an optimal combination for the following computations. This computation was carried out on a personal computer

Table 1. Gas phase governing equations

$$\frac{\partial}{\partial t}(\rho\phi)+\frac{\partial}{\partial x}\left(\rho u\phi-\Gamma\frac{\partial\phi}{\partial x}\right)+\frac{\partial}{\partial y}\left(\rho v\phi-\Gamma\frac{\partial\phi}{\partial y}\right)=S$$

Equation	ϕ	Γ	S
Continuity	1	–	0
x-momentum	u	$\frac{\mu}{\sqrt{\mathrm{Gr}}}$	$\frac{\partial P}{\partial x}+S_u$
y-momentum	v	$\frac{\mu}{\sqrt{\mathrm{Gr}}}$	$\frac{\partial P}{\partial y}+S_v+\frac{\rho_\infty-\rho}{\rho_\infty-\rho_f}$
energy	T	$\frac{\mu}{Pr.\sqrt{\mathrm{Gr}}}$	$-q\cdot\dot{\omega}_F$
fuel	Y_F	$\frac{\mu}{Pr.\sqrt{\mathrm{Gr}.\mathrm{Le}}}$	$\dot{\omega}_F$
oxidizer	Y_O	$\frac{\mu}{Pr.\sqrt{\mathrm{Gr}.\mathrm{Le}}}$	$f\cdot\dot{w}_F$

$S_u=\frac{1}{3}\frac{\partial}{\partial x}\left(\frac{\mu}{\sqrt{\mathrm{Gr}}}\frac{\partial u}{\partial x}\right)+\frac{\partial}{\partial y}\left(\frac{\mu}{\sqrt{\mathrm{Gr}}}\frac{\partial v}{\partial x}\right)-\frac{2}{3}\frac{\partial}{\partial x}\left(\frac{\mu}{\sqrt{\mathrm{Gr}}}\frac{\partial v}{\partial y}\right)$
$S_v=\frac{1}{3}\frac{\partial}{\partial y}\left(\frac{\mu}{\sqrt{\mathrm{Gr}}}\frac{\partial v}{\partial y}\right)+\frac{\partial}{\partial x}\left(\frac{\mu}{\sqrt{\mathrm{Gr}}}\frac{\partial u}{\partial y}\right)-\frac{2}{3}\frac{\partial}{\partial y}\left(\frac{\mu}{\sqrt{\mathrm{Gr}}}\frac{\partial u}{\partial x}\right)$

at National Chiao Tung University. The execution time for a typical case was about 45–60 minutes.

RESULTS AND DISCUSSION

In order to make a fair comparison, the selected solid fuel, a cellulosic material of 2.5 mm thickness, was chosen. This material is exactly the same used by Lin and Chen (2000). All related properties describing the gas-phase chemical reaction and solid-fuel pyrolysis process can refer to Lin and Chen (2000). The imposed Gaussian radiant heat flux, whose half-width is 1-cm wide (corresponding to 7.2 nondimensionally), is also the same as that given in the last reference, except that the incident orientation was vertically downward. A presentation of the ignition behavior over a horizontal fuel is given first; the discrepancy between the horizontal and the vertical cases is depicted as well. A parametric study based on a change in gravity level follows.

Radiative Ignition Process

Figure 2 is the maximum temperature history in the computational domain for vertical and horizontal solid fuels. Similar to the classification for vertically oriented solid fuel ignition behaviors defined by Lin and Chen (2000), the entire process can be divided into two distinct stages according to the relationship between the maximum temperature and

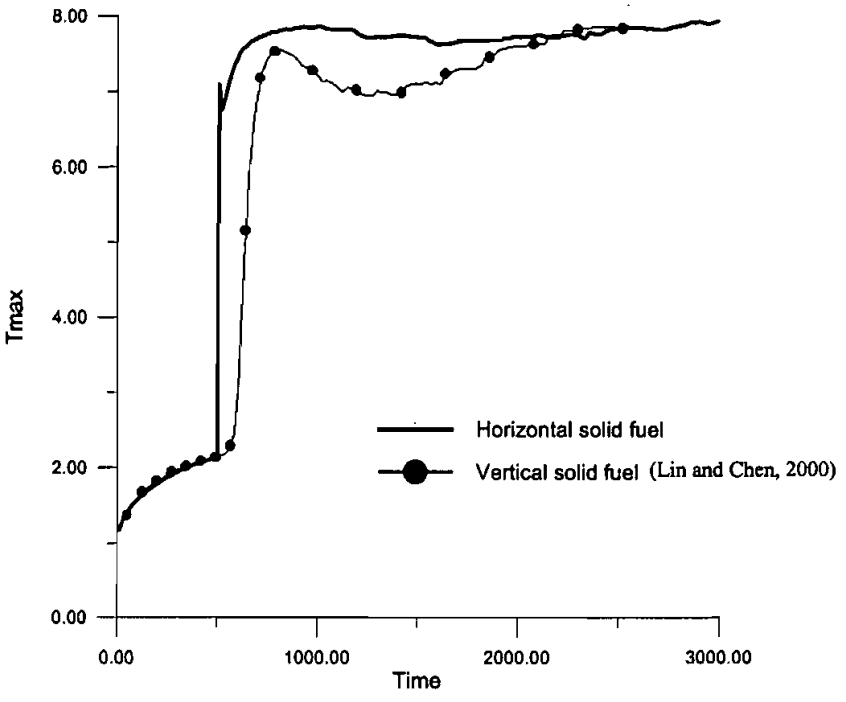

Figure 2. Temporal variation of maximum temperature (T_{max}) in the computational domain for horizontally and vertically oriented solid fuels.

time, as shown in this figure. They are (1) the heating-up stage and (2) the flame-development stage. The first stage begins when the external radiative heat flux starts to impose on the fuel surface and ends as the ignition is ready to occur. Ignition initiation is defined as the instant when the specified fuel reaction rate, 10^{-4} g/cm^3.s (suggested by Ferkul and T'ien [1994] and Nakabe et al. [1994]), first appears in the gas phase. The flame-development stage includes both the ignition (thermal run away) and transition processes. The ignition process commences with ignition initiation. The transition process starts when the maximum temperature in the gas phase reaches its highest value in the ignition process.

Stage 1 is the heating-up stage and its time interval is $0 \leq t < 410$, in which the upper boundary is the time for ignition initiation. Cases (*a*) to (*d*) in Figures 3 to 5 demonstrate this process. Figure 2 reveals that the maximum temperature increases with time during this stage. The duration, 410, is defined as ignition delay time (IDT) for the specified conditions.

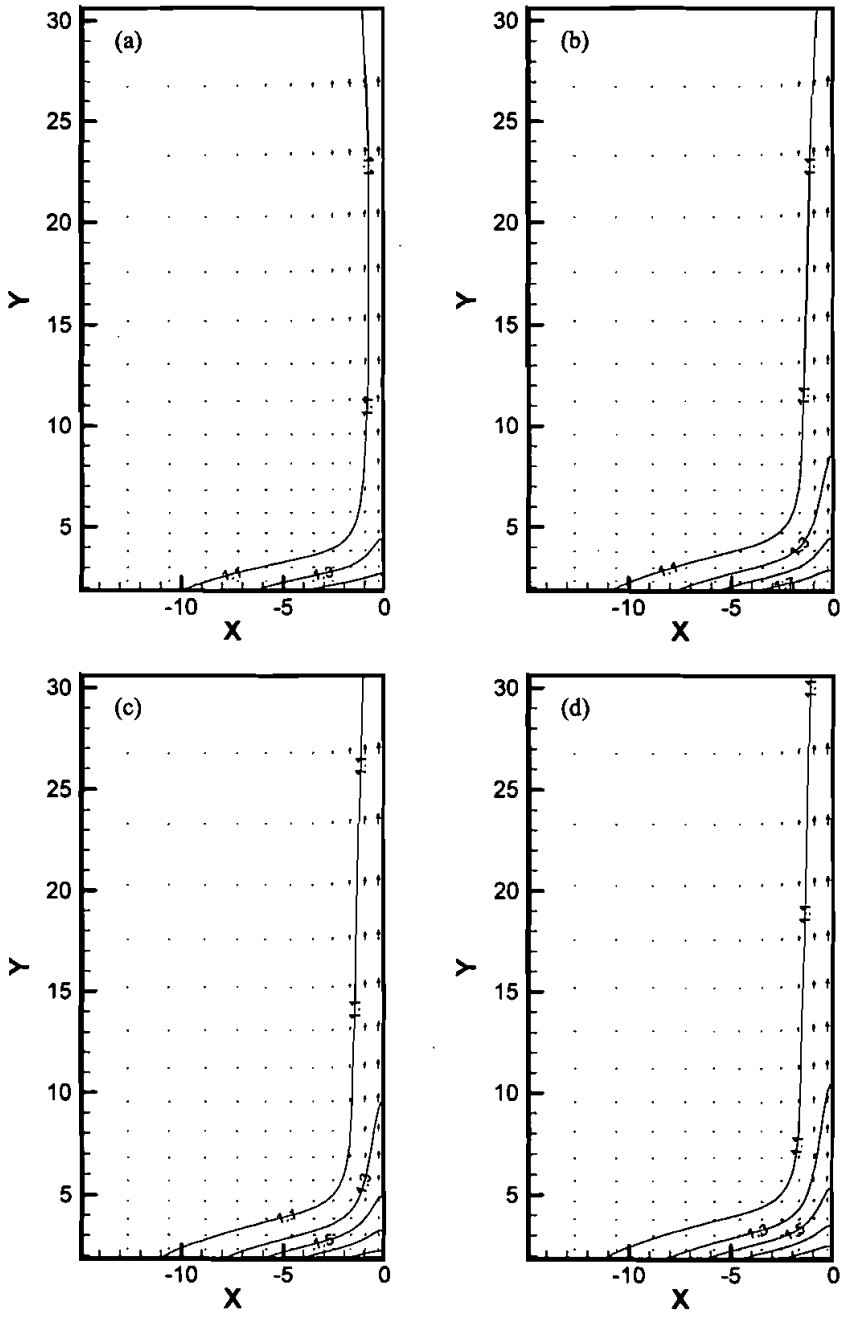

Figure 3. Isotherm and velocity vector distributions for (*a*) $t = 150$ (*b*) $t = 300$ (*c*) $t = 350$ (*d*) $t = 400$ (*e*) $t = 410$ (*f*) $t = 470$ (*g*) $t = 510$ (*h*) $t = 2000$.

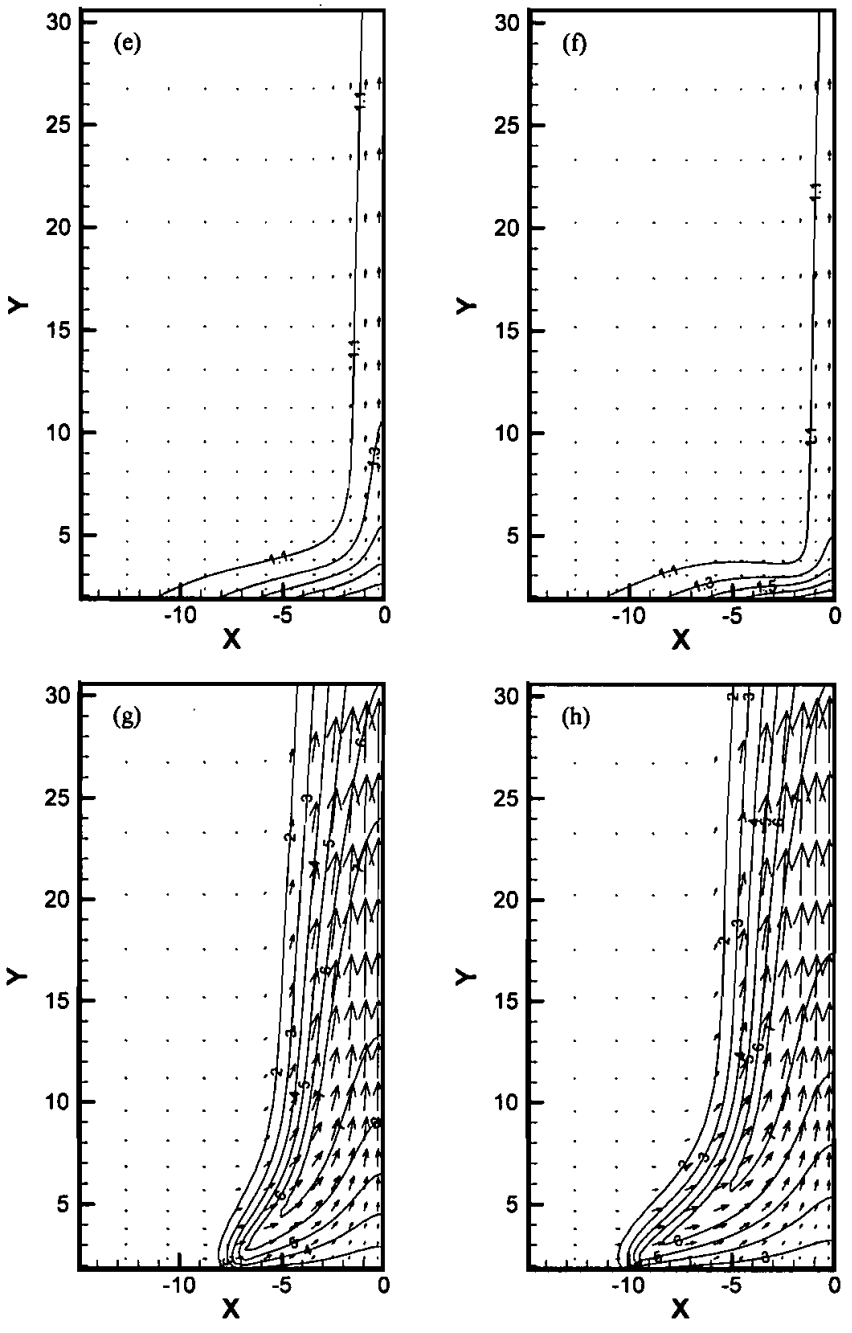

Figure 3. (Continued).

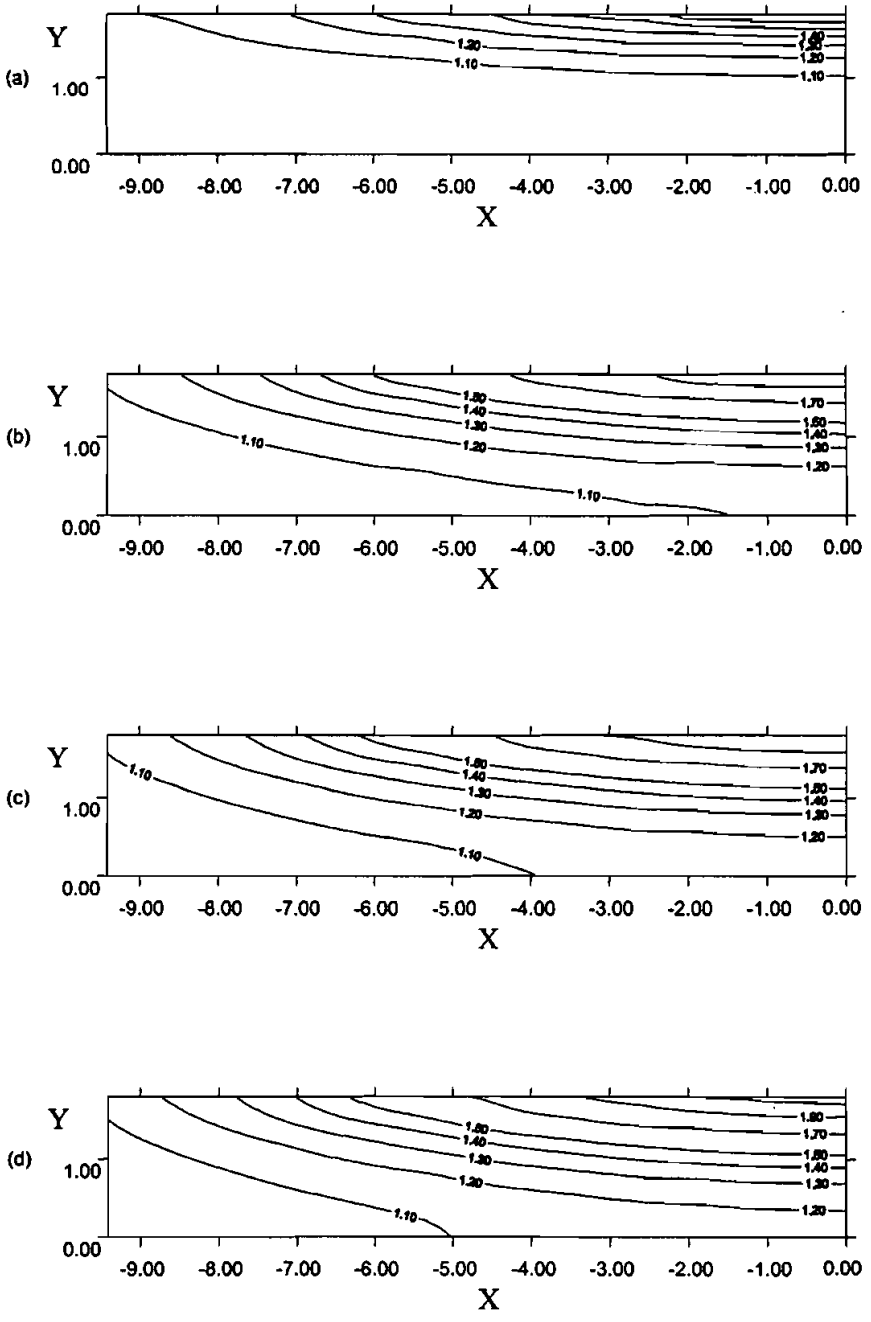

Figure 4. Solid fuel temperature distribution of horizontal solid fuel for (*a*) $t = 150$ (*b*) $t = 300$ (*c*) $t = 350$ (*d*) $t = 400$ (*e*) $t = 410$ (*f*) $t = 470$ (*g*) $t = 510$ (*h*) $t = 2000$.

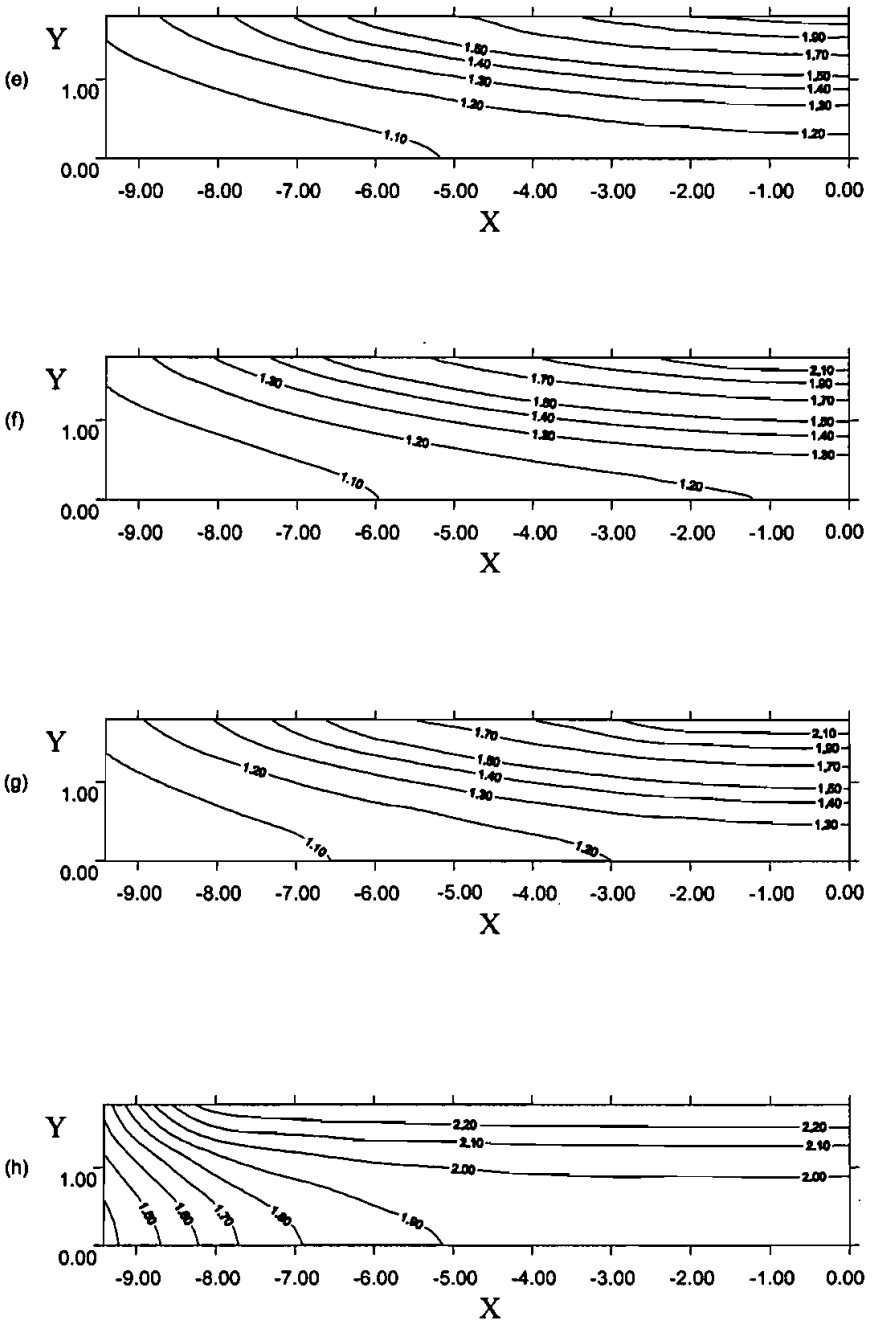

Figure 4. (Continued).

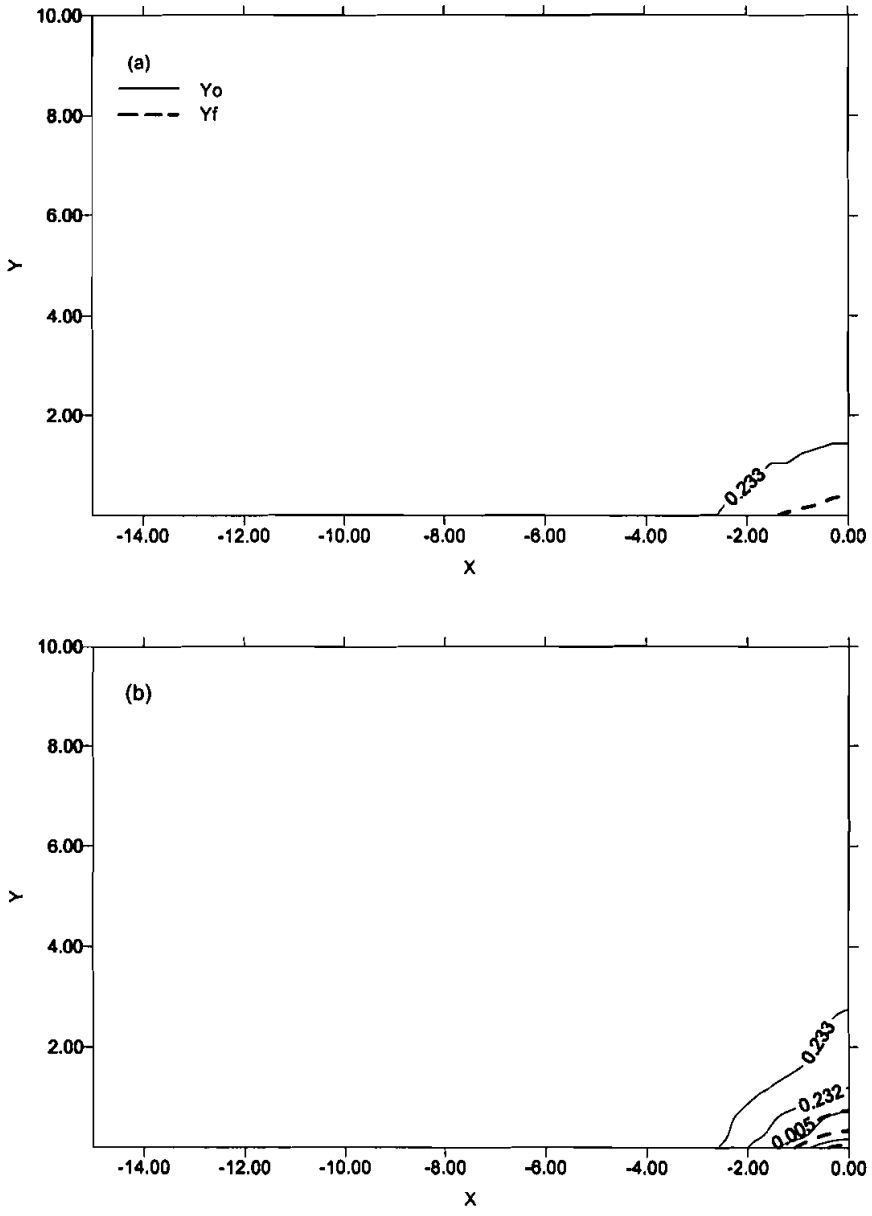

Figure 5. Fuel and oxygen mass fraction contours for (a) $t = 150$ (b) $t = 300$ (c) $t = 350$ (d) $t = 400$ (e) $t = 410$ (f) $t = 470$ (g) $t = 510$ (h) $t = 2000$.

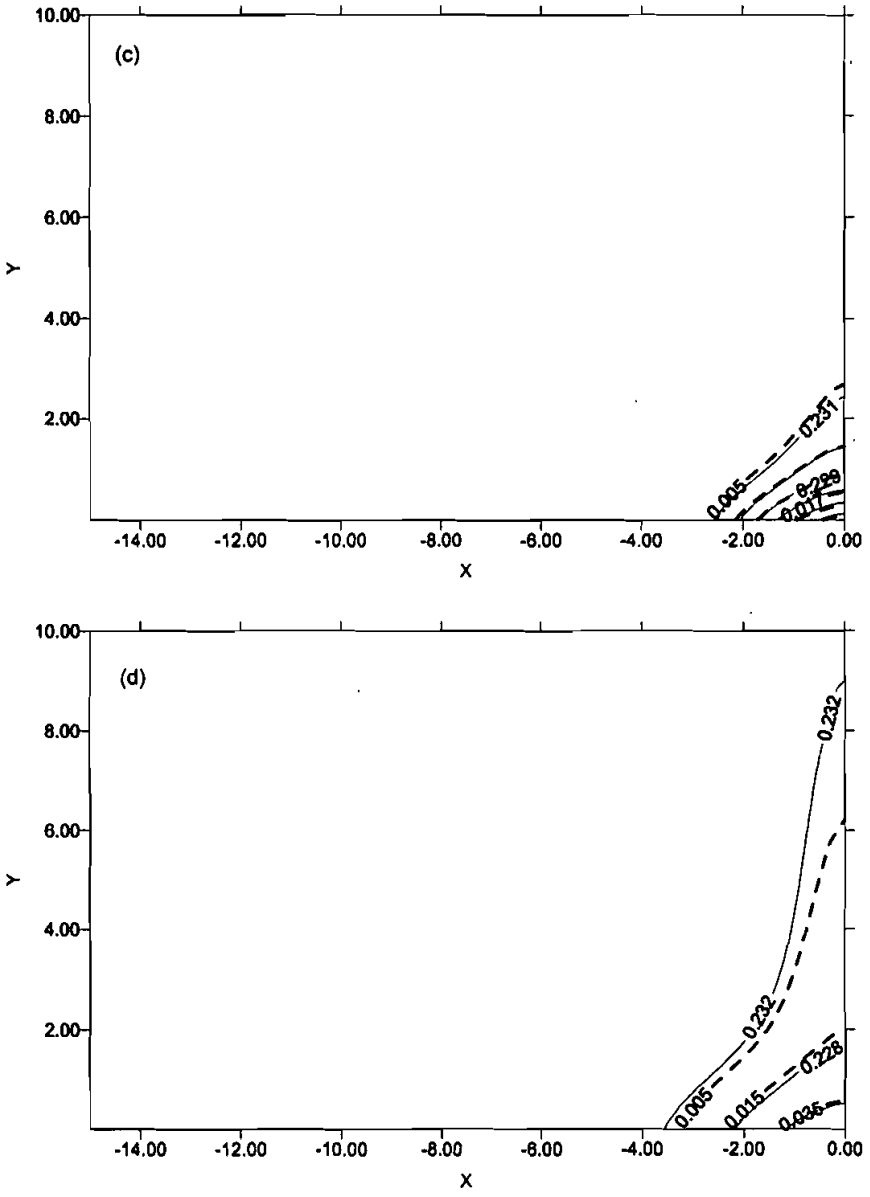

Figure 5. (Continued).

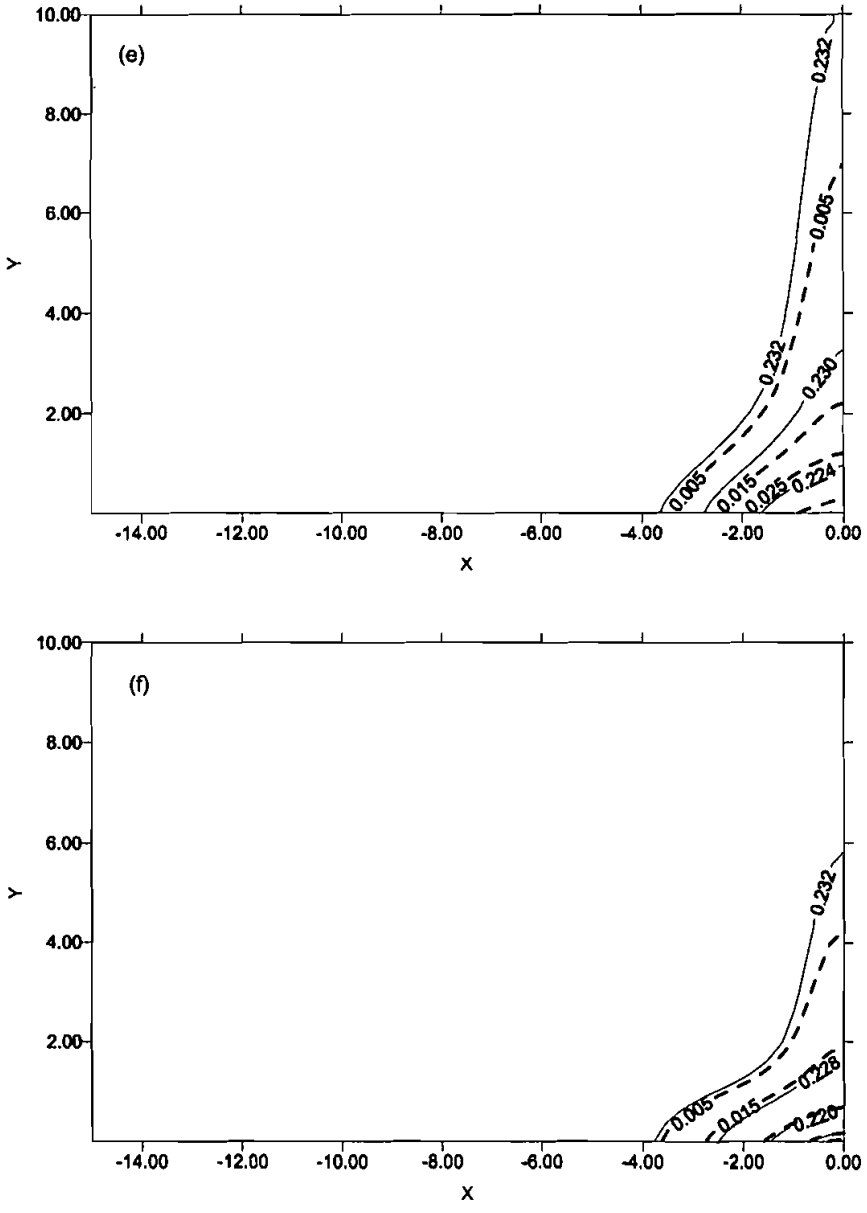

Figure 5. (Continued).

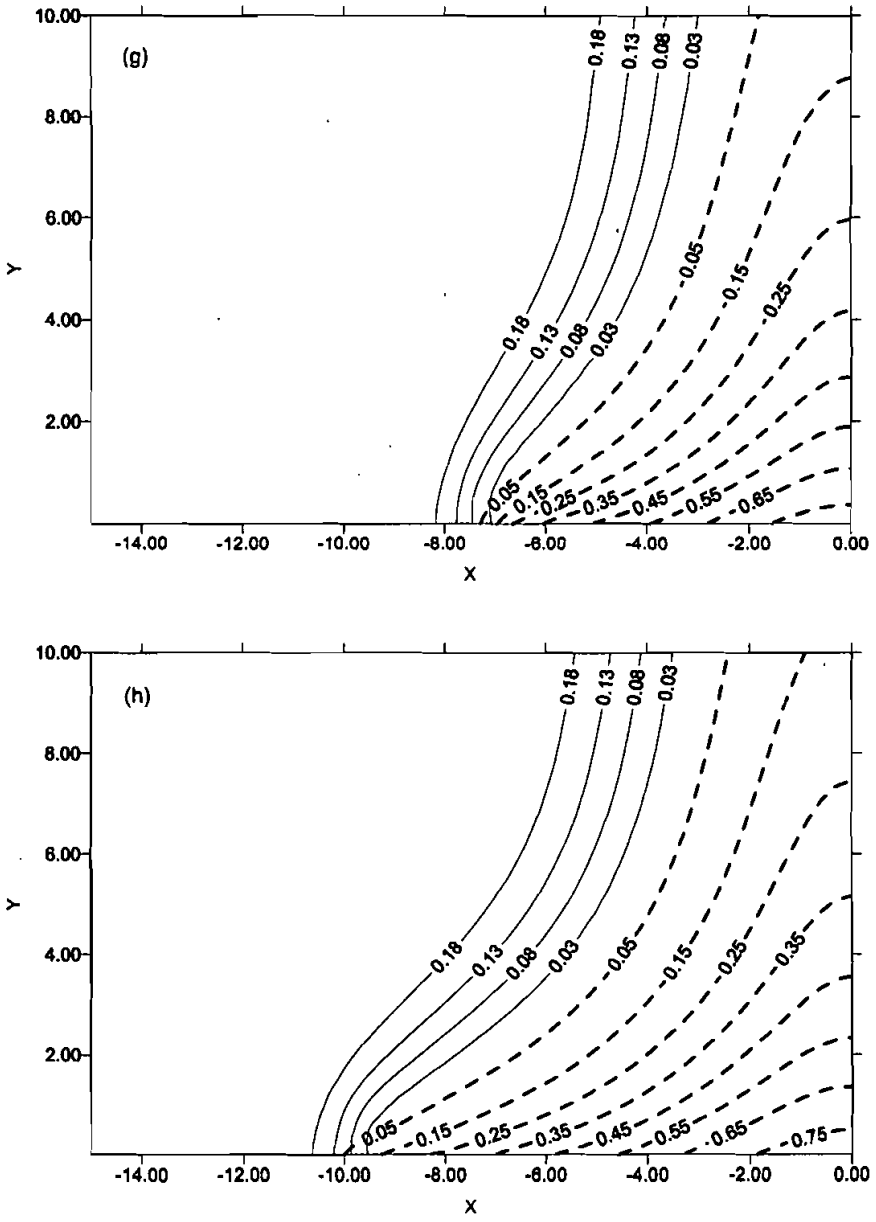

Figure 5. (Continued).

The heated region is defined as the area in the gas or solid phase that is enclosed by an isotherm equal to or greater than 1.1. During the heating stage, Figures 3(*a*) to (*d*) show that the heated region in the gas phase expands with time as a result of continuous heating. The expansion in the lateral $(-x)$ direction is faster than that in the vertical $(+y)$ direction. This implies that the natural convection is not significant enough in this stage and that the gas-phase conduction heat transfer in the lateral direction is reinforced by heat transfer through the solid.

In Figure 3(*a*) ($t = 150$), the induced flow is still not yet apparent (the maximal nondimensional velocity is 1.303 at this instant). The temperatures are found to decrease in the $-x$ direction, because the heat flux imposed at the interface is in a Gaussian distribution and its peak is located at $x = 0$. The nondimensional length of the heated region in the x-direction is about 10. At $t = 300$ (Figure 3[*b*]), it can be seen that the heated region expands faster in the y-direction than in the x-direction. The temperature distributions are now strongly affected by the induced-flow motion. The entrained air at ambient temperature moves horizontally toward the symmetry line ($x = 0$) and cools the heated gas, i.e., convection is opposite to conduction. On the other hand, the heated gas moves upward due to buoyancy, and convection is concurrent with conduction.

In the present simulation, the flow structure is affected mainly by the following factors: the buoyant force, viscous effect, and thermal expansion effect. As shown in Figure 3(*b*) ($t = 300$), the buoyant force, which moves in a direction perpendicular to solid fuel surface, provides the potential for upward $(+y)$ flow motion and simultaneously results in the entrainment of ambient air. This upward movement can only be sustained as long as the buoyancy remains stronger than the viscous effect. Before the flow becomes almost quiescent, the thermal expansion causes the flow to deflect outward $(-x)$. A similar flow structure was also found in the following heating process (Figure 3[*c*]–[*d*]). The maximal nondimensional induced velocity increased substantially from 1.303 at $t = 150$ to 2.186 at $t = 400$. This is mainly because the buoyant force is strengthened by the increasing temperature gradient in the gas phase.

For the corresponding solid fuel temperature distributions, Figures 4(*a*) to 4(*d*) show that the heated region increases with time as well. The heat penetration depth is defined as the vertical length measured from the interface up to where $T_s = 1.1$. The compound results show that it is 1.8 nondimensionally at $t = 300$. Before t = 300, see Figure 5(*a*), the

maximal heat penetration depth is located at $x = 0$. As shown in Figure 5(c), heat diffusion leads to the isothermal line of $T_s = 1.1$, farther away from $x = 0$ at the insulated boundary. Also note that the temperature gradient in the y-direction decreases laterally. These phenomena are attributed to the external heat flux being in a type of Gaussian distribution with its peak located at $x = 0$.

At $t = 350$, the maximal temperature in the gas phase is now 2.004, located at $x = -0.1$ and $y = 1.8$, which is greater than the maximum at the interface, $T_s = 2.0$. This is the first instance in which the temperature gradient at the interface becomes positive, indicating that the solid has started to receive energy from the hotter gas. Of course, the appearance of hotter gas also implies that the chemical reaction is now triggered in the gas phase. However, this area is very small. Apparently, this reaction is insignificant and not strong enough for ignition. At $t = 400$, the time step just before ignition occurs, the maximal gas-phase temperature becomes 2.056, whereas the maximum at the interface is 2.012. The difference is greater now due to heat generation by the gas-phase chemical reaction. Generally speaking, the maximal temperature occurs at the interface during the majority of the heating-up stage. The average rate of increase is about 281.5 K/s.

The corresponding fuel/oxygen mass fraction distributions in this heating stage are shown in Figures 5(a) to (d). It can be seen that the frontier of the generated fuel vapor contours expands with time. The maximal fuel-mass fraction, occurring at the interface, increases from 7.70×10^{-5} at $t = 150$ to 0.0559 at $t = 400$, implying that the volatiles are accumulating near the pyrolyzing surface. From these distributions, diffusion is apparently enhanced by convection, due to blowing in the volatile generation process. In the mixing process, a combustible, premixed fuel/oxygen mixture is gradually formed. At $t = 400$, the fuel-to-oxygen ratio mass fraction in the mixture is about 0.158 at the region near $x = 0$, just above the fuel surface. It is now in preparation for the following ignition.

The flame-development stage comes after the heating-up stage. This consists of the ignition and transition processes. The period between $t = 410$ to $t = 510$ is classified as the ignition process, which starts from $t = 410$ as the initiation of ignition. A sharp increase in gas-phase maximal temperature marks this ignition process. It increases from 2.065 to 7.096 within 0.5777 seconds. The average rate of increase is about 2612.6 K/s, much greater than that in the heating-up stage.

Figure 6 shows several flames at specified instances to illustrate their growth history during the ignition process. The flame boundary is marked

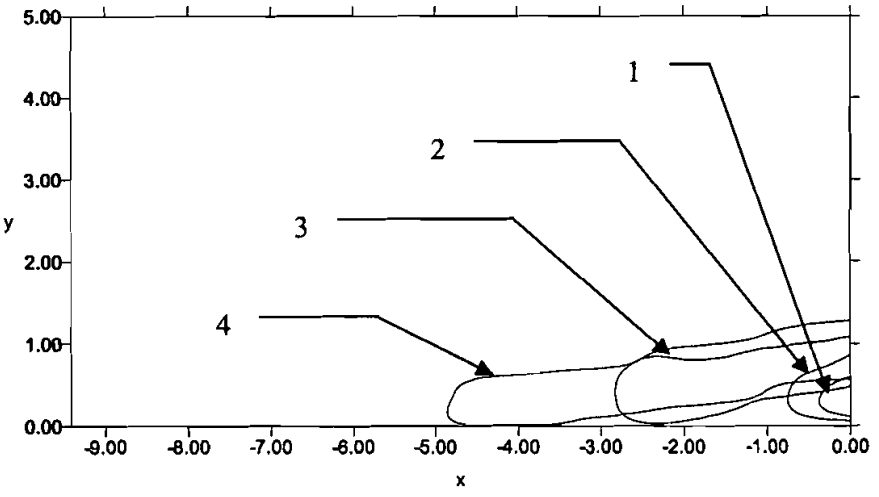

Figure 6. Constant contour levels of the chemical reaction rate equal to 10^{-4} g/cm^3/s at various time (1:$t = 410$, 2:$t = 420$, 3:$t = 470$; 4:$t = 510$).

by $|\omega_F| = 10^{-4}$ g/cm^3/s as mentioned previously. It is evident that the flame grows very quickly from an initially smaller, weaker flame (marked by 1) to a much larger, stronger flame (marked by 4) within 0.5777 second in this process. This sudden flame development is caused by a combustion wave front propagated through the combustible mixture that can be seen in detail in Figures 3(*e*) to 3(*g*). The premixed fuel/oxygen mixture is ignited and reaches a higher gas-phase temperature through the heat released in the chemical reaction. The increased heat, in turn, further accelerates the chemical reaction, which generates more heat. This is why the maximal temperature increases so sharply in this process.

This sudden gas expansion further accelerates the upward motion. The maximal velocities at $t = 410$ and $t = 470$ are 2.236 and 3.573, respectively. At $t = 510$, the velocity reaches 4.484. This acceleration is quite significant. On the other hand, the induced flow ahead of the flame's leading edge is retarded, as shown in the same figures, because it is subjected to an adverse pressure gradient. This pressure gradient is caused by a local high-pressure plateau generated by thermal expansion due to the active combustion.

Figures 5(*e*) to (*g*) depict how the contours of the oxygen mass fraction are pushed outward, owing to its own consumption by reaction with

time. In the neighborhood of the pyrolyzing surface, only fuel vapors can exist. This is because the ambient oxygen cannot penetrate through the active reaction zone and the fuel is continuously supplied via the interface. Up to $t = 510$ (Figure 5[g]), the end of the ignition process and the beginning of transition one, the flame starts to show the characteristics of a diffuse flame. However, a small region containing a premixed mixture is still found to exist just ahead of the flame front. This is attributed to both the fuel and oxidizer leaking through the quenching layer between the flame front and solid-fuel surface to form a fuel-oxidizer mixture. This mixture serves as a continuous ignition source for further flame propagation.

The growing flame also contributes to solid-fuel heating. The energy provided by the flame reinforces the gradual decay of the radiant energy supply at the upstream end, due to Gaussian distribution. Therefore, the positions of the $T_s = 2.1$ isothermal line fronts in Figures 4(f) and 4(g) become nearly the same as the corresponding flame fronts shown in Figure 6.

The transition process comes immediately after the ignition process. The flame now propagates outward along the solid fuel. It starts from $t = 510$, when the gas phase temperature reaches the maximum, of $T = 7.096$. After that, it decreases from this value sharply, as a large amount of the premixed mixture is consumed almost completely. During this process, the maximum temperature in the gas phase decreases to a minimum, 6.751, at $t = 520$. The temperature then oscillates and increases again, as illustrated in Figure 2. The oscillation of the maximal gas phase temperature seems to have a connection with the lag between the flame and pyrolysis fronts, as shown in Figure 7. This phenomenon will be discussed later. By comparing the structures in the flame front area at $t = 510$ and $t = 2000$, we can see that they are quite similar, except for the location due to flame spread.

Figure 7 illustrates the flame- and pyrolysis-front positions as functions of time. The position of the pyrolysis front is defined as the upmost location of $\rho_s = 0.99$ along the fuel surface. When $t < 400$, the pyrolysis front is ahead of the flame one, as a result of the continuous heating from the external radiation. After the initiation of ignition, $t = 410$, the flame front extends quickly. At $t = 510$, the end of the ignition process, the flame front catches up with the pyrolysis front. In the transition process, the flame continuously propagates upstream. During the spreading process, the volatiles diffuse and convect away

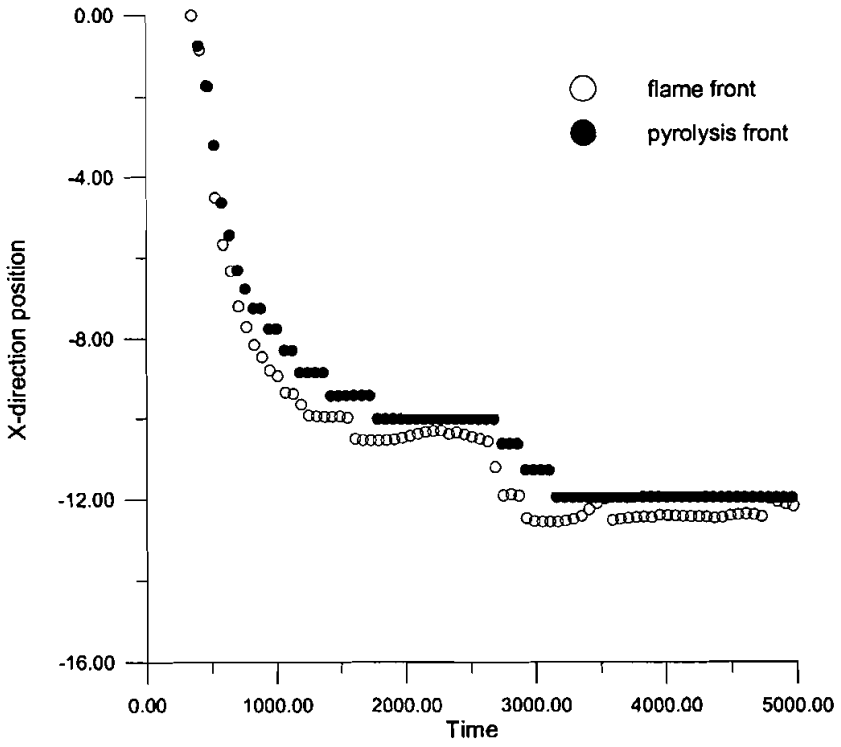

Figure 7. Flame front and pyrolysis front positions for horizontal solid fuel.

from the surface. Most volatiles diffuse into the reaction zone and react with the oxidizer to generate heat to sustain the flame itself, while others mix with the oxidizer to form a flammable mixture ahead of the flame leading edge. Subsequently, this mixture is ignited by the trailing flame front to move the flame forward. Therefore, the flame front always overtakes the pyrolysis front in this process. A similar trend was also observed in the experiment by Ito and Kashiwagi (1986). Furthermore, in Figure 7, the flame front exhibits an oscillatory behavior after $t = 1000$ and becomes more obvious with increasing time. This is because the solid fuel does not produce enough fuel vapors ahead of the flame to let the flame propagate. The flame, therefore, must retreat to obtain more fuel vapors from downstream. The flame spread becomes unstable. This oscillatory behavior was also found in the experiment by Olson (1987), who used a thermally thin fuel. It can also be seen that a

lag exists between the flame and pyrolysis fronts in this process. At $t = 410$, the flame front is just a little ahead of the pyrolysis front. However, at $t = 720$, the flame region extends further upstream in the $-x$ direction, while the pyrolysis front still remains at nearly the same position. This indicates that a flammable mixture is being built up as it is completed and then ignited by the flame front. The flame front moves forward instantly and waits for the establishment of the next flammable mixture to propagate itself again.

According to the formula summarized by Fernandez-Pello (1995), the time required for the surface temperature to reach the pyrolysis temperature can be expressed as: $\bar{t}_p = \pi \bar{k}_s \bar{\rho}_s \bar{c}_s (\bar{T}_p - \bar{T}_o)^2 / 4\bar{q}_f''^2$. Note that this formula is applicable only for thermally thick solid fuels with an insulated boundary. If T_p is taken as 700 K (the ceiling pyrolysis temperature) and $\bar{q}_f''$ is taken as the peak heat flux ahead of the flame front, then the time required to reach the pyrolysis temperature is 10.832 s. This time scale can also be regarded as the build time for the flammable mixture in front of the flame front. On the other hand, the characteristic time for the flow field is 5.548×10^{-3} s (obtained by reference length/reference velocity; Lin and Chen [2000]). Apparently, the gas-phase reaction time is much shorter than the pyrolysis time, which is the main cause for this lag.

Effect of Solid Fuel Orientation on Ignition Characteristics

When the solid fuel is subjected to a radiant heat flux in a quiescent environment, the heated solid will transfer energy to the gas layer adjacent to the surface, which causes the temperature of the solid to rise. This leads to a change in the density of the solid-fuel surface, resulting in a natural convection nearby. The interaction between the fuel surface and buoyant flow motion depends on the solid-fuel orientation. Since the induced flow fields are quite different between horizontal and vertical solid fuels, it is expected that the ignition behaviors for both orientations should be different as well (see Figure 2 for an example).

Table 2 lists the computed results for the vertical and horizontal ignition modes. It shows that the ignition delay time is shorter for a horizontal solid fuel than for a vertical one under the same external radiant flux. This trend is consistent with that observed in the experimental works by Kashiwagi (1982). A physical interpretation of this

Table 2. Effect of solid fuel orientations on ignition characteristics

Computed results / Mode	Ignition delay time(s)			T_{simax}(interface maximum temperature at ignition)		
	PEAK FLUX $= 3.5$ w/cm^2 (Case 1)	PEAK FLUX $= 5$ w/cm^2 (Case 2)	PEAK FLUX $= 6.5$ w/cm^2 (Case 3)	PEAK FLUX $= 3.5$ w/cm^2 (Case 1)	PEAK FLUX $= 5$ w/cm^2 (Case 2)	PEAK FLUX $= 6.5$ w/cm^2 (Case 3)
Horizontal	4.9840	2.2455	1.2597	2.023	2.058	2.081
Vertical	9.749	4.217	2.246	2.22	2.26	2.29

phenomenon will be given in detail next. Case 2, with a peak heat flux of 5 W/cm^2 in Table 2, was selected as a reference case to explore the orientation effect on solid-fuel ignition behavior.

In Figure 8(*a*), the fuel is in a horizontal mode. In the upstream ($-x$), the heat conduction moves against the incoming cold convection. However, the convection near the symmetrical plane rises upward due to the impingement of two equal-strength but opposed convective flows at the $x = 0$ plane. The volatiles from the pyrolyzing surface are injected into the flow field. A symmetrical thermal plume is then formed. Since the peak heat flux of the Gaussian distributions are centered at $x = 0$ and the

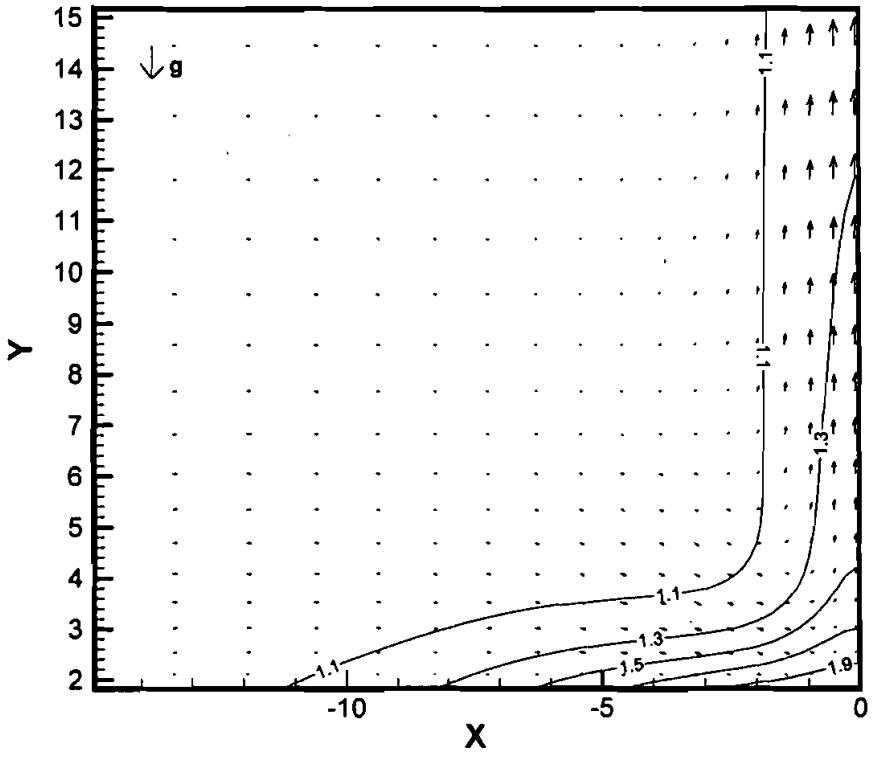

Figure 8. Comparison of solid fuel orientations on heating process at $t = 410$. (*a*) Isotherm and velocity vector distributions for horizontal solid fuel. (*b*) Horizontal solid fuel temperature distributions. (*c*) Horizontal solid fuel density distributions (contour values: 0.99, 0.998). (*d*) Isotherm and velocity vector distributions for vertical solid fuel. (*e*) Vertical solid fuel temperature distributions. (*f*) Vertical solid fuel temperature distributions.

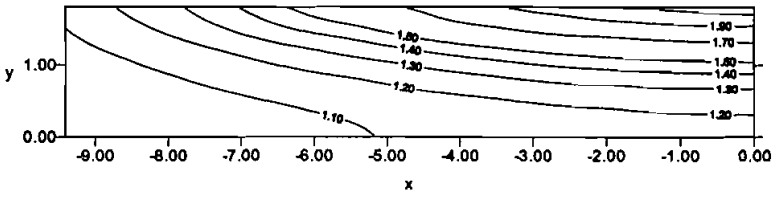

Figure 8(*b*).

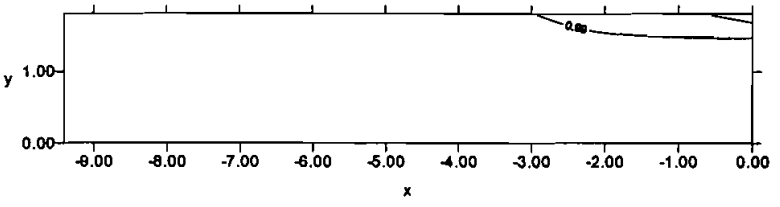

Figure 8(*c*).

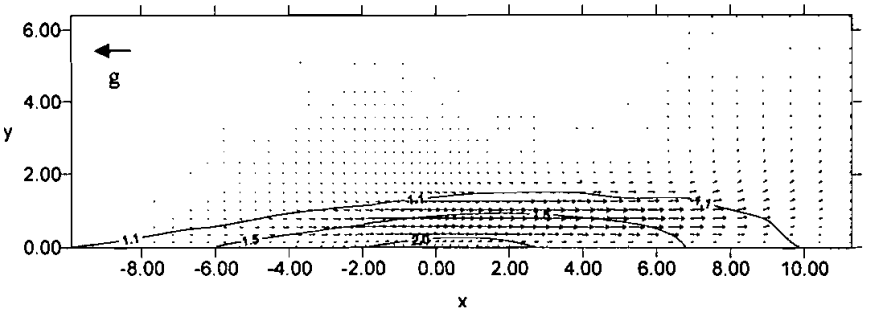

Figure 8(*d*).

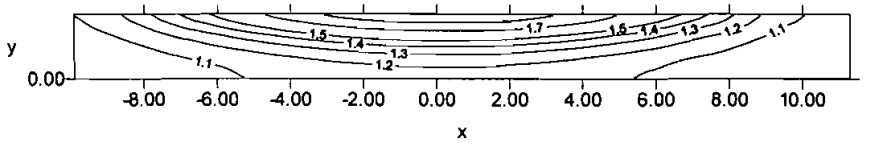

Figure 8(*e*).

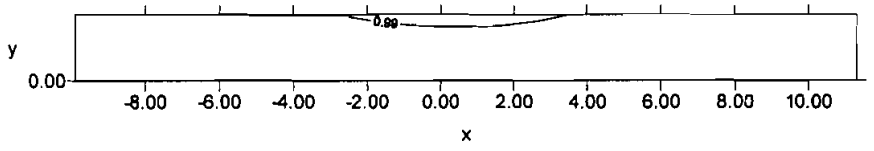

Figure 8(*f*).

temperature in the vicinity of $x = 0$ and $y = 0$ is not cooled by the induced flow, the highest temperature region in the flow field is located at that point. The gas-phase temperature profiles show a similar shape as the Gaussian heat flux distributions. Therefore, a chemical reaction is indicated in the gas phase, causing a heat release.

In the vertical mode, the buoyant force is in a direction parallel to the solid-fuel surface. As shown in Figure 8(*d*), the upstream heat conduction is also against the incoming induced flow, whereas downstream it is concurrent with the heat convection. Therefore, the initially symmetrical condition with respect to $x = 0$ no longer exists. Now the highest temperature region shifts downstream from $x = 0$ and the heated area in the gas phase now becomes larger downstream. A thermal plume is formed as well.

From the characteristics of these two flow fields, the upstream heat, carried by convection, accumulates in the middle plane of $x = 0$ due to the stagnation plane. This results from impingement in the horizontal mode. In the vertical mode, the heat is carried downstream directly and no mechanism for heat accumulation exists. In the meantime, a similar behavior is applied for the flammable mixture, made up of the fuel vapors and oxidizer (see Figures 8[*a*] and [*b*]). The flammable mixture is also easier to build up in horizontal mode. Therefore, under the same incident heat flux, the temperature rise in the solid fuel is expected to occur faster in the horizontal mode and, consequently, so does ignition.

This can be confirmed from the maximum temperature being located at the interface with a value of 2.157 at $t = 410$ for vertical solid fuel. At the same time, ignition occurs for a horizontal solid fuel when the gas-phase maximum temperature is 2.236. As to the interface maximum temperature at ignition, both cases (vertical and horizontal modes) show that the maximum interface temperature increases in the external heating rate. Figures 8(*a*) and (*d*) depict a gas phase heated lengthwise in the x-direction that is nearly the same for the two modes. In the y-direction, the

maximal heated length for the horizontal solid fuel is much greater than for the vertical one.

Table 2 also indicates that the ignition delay-time difference between the horizontal and vertical solid fuels increases with a decrease in the external heating rate. Since the lower heating rate increases the ignition delay time, the flow effect becomes more significant. It is expected that the magnitude of the ignition delay-time difference increases with a decrease in the heating rate.

Gravity Level Effect on Ignition Characteristics

Changes in gravity level affect the buoyant force potential and, in turn, the induced flow motion. From the analysis given above, the resultant temperature and fuel/oxygen mass fraction distributions are dominated by the gravity level. Therefore, it is expected that the ignition behavior will be influenced by the change in gravity. Table 3 lists the ignition delay times and maximal temperatures at the interface at ignition as a function of the gravity level. It shows that the ignition delay time increases with an increase in gravity level. The interface maximal temperature at ignition shows a similar trend. This is because the greater flow velocity induced in a higher-gravity environment causes more heat loss to the environment. In the meantime, the heat-accumulation region near the symmetry line is contracted due to stronger opposed flow. Nakamura, Yamashita, and Takeno (2000) also predicted the same trend for thin-solid fuel.

CONCLUSIONS

A theoretical analysis was developed and solved numerically to study the ignition behaviors of a horizontally oriented cellulosic material under

Table 3. Effect of gravity level on ignition characteristics

g	Ignition delay time(s)	T_{simax}
0.25	2.0081	2.05
0.5	2.1035	2.05
0.75	2.1231	2.05
1	2.2455	2.0583
2	2.3462	2.0636
3	2.4750	2.0664
4	2.5161	2.0677

natural convection conditions in a normal gravitational field. The governing system for the gas phase consisted of the following components: a set of time-dependent conservation equations for the continuity, momentum, energy, and species; an equation of state; an expression of viscosity variation with temperature; and a one-step overall chemical reaction with finite-rate global kinetics. The above equations were coupled with the unsteady solid-phase energy and mass conservation equations at the interface.

The ignition and transition to flame-spread process over the solid fuel can be divided into two stages: the heating-up stage and the flame-development stage. During the heating-up stage, the maximum temperature, occurring at the interface, increases with time. In the heating process, the heated region expands apparently more in the y-direction than in the x-direction. It is affected mainly by flow motion. A flammable mixture for the following ignition is generated. Also, the maximum induced flow velocity increases with time because of the increasing temperature gradient. The flame-development stage includes both the ignition and transition processes. The ignition process is marked with a sharp increase in the maximum temperature. This is because a large amount of heat is generated from the chemical reaction in the accumulated flammable mixture. In the meantime, the flame is in transition from a premixed to a diffused flame, except for a small region just around the flame front. The induced flow ahead of the flame's leading edge is retarded by the local high-pressure plateau generated by the thermal expansion attributable to active combustion. In the transition process, the flame continuously spreads out. Since there is a time lag between solid-fuel pyrolysis and the gas phase chemical reaction, the pyrolysis front overtakes the flame front in the initial heating-up process. Once the situation in the vicinity of the flame front reaches ignition status, the flame moves forward quickly and the flame front then moves ahead of the pyrolysis front. This is the so-called opposed flame spread, in which the flame serves as a pilot and heat source to provide heat to increase the gas and solid-phase upstream temperatures.

The solid-fuel orientation effects (horizontal and vertical) on the radiative ignition characteristics were compared. The ignition delay times were shorter for horizontal than for vertical solid fuel under the same external heat flux. This is because the high temperature region was not cooled and the resultant flammable mixture was not diluted by the induced flow as with a horizontal solid fuel. In addition, the magnitude of

the ignition delay time difference between the vertical and horizontal modes, subjected to the same incidence of heat flux, increased with a decrease in the external heating rate. The computed results also show that the ignition delay time decreased with a decrease in gravity level, because the larger flow velocity induced in a high-gravity environment.

REFERENCES

Chen, C.H. and Yang, M.T. (1998) Numerical analysis of flame spread over a thin fuel inclined from vertically downward to horizontal. *Journal of the Chinese Society of Mechanical Engineering*, **19**, 397–410.

Duh, F.C. and Chen, C.H. (1991) A theory for downward flame spread over a thermally thin fuel. *Combustion Science and Technology*, **77**, 291–305.

Ferkul, P.V. and T'ien, J.S. (1994) A model of low-speed concurrent flow flame spread over a thin fuel, *Combustion Science and Technology*, **99**, 345–370.

Fernandez-Pello, A.C. (1995) The solid phase. *Combustion Fundamentals of Fire*. (G. Cox, Ed.), pp. 34–100, Academic Press, Inc., San Diego, CA.

Ito, A. and Kashiwagi, T. (1986) Temperature measurements in PMMA during downward flame spread in air using holographic interferometry, *Twenty-First Symposium (International) on Combustion*. The Combustion Institute, Pittsburgh, PA, pp. 65–74.

Kashiwagi, T. (1982) Effect of sample orientation on radiative ignition. *Combustion and Flame*, **44**, 223–245.

Lin, P.H. (1999) The study of ignition and flame spread over a thick solid fuel. Ph.D. Diss., Department of Mechanical Engineering, National Chiao-Tung University, Hsin Chu, Taiwan, p. 300.

Lin, P.H. and Chen, C.H. (2000) Numerical analyses for radiative autoignition and transition to flame spread over a vertically oriented solid fuel in a gravitation field. *Combustion Science and Technology*, **151**, 157–187.

Mcgrattan, K.B., Kashiwagi, T., Baum, H.R. and Olson, S.L. (1996) Effect of ignition and wind on the transition to flame spread in a microgravity environment. *Combustion and Flame*, **106**, 377–391.

Nakabe, K., Mcgrattan, K.B., Kashiwagi, T., Baum, H.R., Yamashita, H. and Kushida, G. (1994) Ignition and transition to flame spread over a thermally thin cellulosic sheet in a microgravity environment. *Combustion and Flame*, **98**, 361–374.

Nakamura, Y., Yamashita, H. and Takeno, T. (2000) Effects of gravity and ambient oxygen on a gas-phase ignition over a heated solid fuel. *Combustion and Flame*, **120**, 34–48.

Olson, S.L. (1987) *The Effect of Microgravity on Flame Spread Over a Thin Fuel*. NASA TM-100195.

Patankar, S.V. (1980) *Numerical Heat Transfer and Fluid Flow*. Hemisphere, London, UK.

West, J., Bhattacharjee, S. and Altenkirch, R.A. (1992) A comparison of the roles played by natural and forced convection in opposed-flow flame spreading. *Combustion Science and Technology*, **83**, 233–244.